The Plant Cell, Vol. 27: 3397–3409, December 2015, www.plantcell.org

KONJAC1 and 2 Are Key Factors for GDP-Mannose Generation and Affect L-Ascorbic Acid and Glucomannan Biosynthesis in Arabidopsis

Shota Sawake,[a] Noriaki Tajima,[a] Jenny C. Mortimer,[b,c,d] Jeemeng Lao,[d] Toshiki Ishikawa,[a] Xiaolan Yu,[b] Yukiko Yamanashi,[a] Yoshihisa Yoshimi,[a] Maki Kawai-Yamada,[a] Paul Dupree,[b] Yoichi Tsumuraya,[a] and Toshihisa Kotake[a,b,1]

[a] Graduate School of Science and Engineering, Saitama University, Saitama 338-8570, Japan
[b] Department of Biochemistry, University of Cambridge, Cambridge CB2 1QW, United Kingdom
[c] Biomass Engineering Program Cooperation Division, RIKEN Center for Sustainable Resource Science, Yokohama 230-0045, Japan
[d] Joint Bioenergy Institute, Emeryville, California 94608

ORCID IDs: 0000-0001-6624-636X (J.C.M.); 0000-0001-9270-6286 (P.D.); 0000-0001-9835-383X (Y.T.); 0000-0002-1110-5006 (T.K.)

Humans are unable to synthesize L-ascorbic acid (AsA), yet it is required as a cofactor in many critical biochemical reactions. The majority of human dietary AsA is obtained from plants. In *Arabidopsis thaliana*, a GDP-mannose pyrophosphorylase (GMPP), VITAMIN C DEFECTIVE1 (VTC1), catalyzes a rate-limiting step in AsA synthesis: the formation of GDP-Man. In this study, we identified two nucleotide sugar pyrophosphorylase-like proteins, KONJAC1 (KJC1) and KJC2, which stimulate the activity of VTC1. The *kjc1kjc2* double mutant exhibited severe dwarfism, indicating that KJC proteins are important for growth and development. The *kjc1* mutation reduced GMPP activity to 10% of wild-type levels, leading to a 60% reduction in AsA levels. On the contrary, overexpression of *KJC1* significantly increased GMPP activity. The *kjc1* and *kjc1kjc2* mutants also exhibited significantly reduced levels of glucomannan, which is also synthesized from GDP-Man. Recombinant KJC1 and KJC2 enhanced the GMPP activity of recombinant VTC1 in vitro, while KJCs did not show GMPP activity. Yeast two-hybrid assays suggested that the stimulation of GMPP activity occurs via interaction of KJCs with VTC1. These results suggest that KJCs are key factors for the generation of GDP-Man and affect AsA level and glucomannan accumulation through the stimulation of VTC1 GMPP activity.

INTRODUCTION

The ability of plants to synthesize L-ascorbic acid (AsA) is critical to human health, since we cannot synthesize it ourselves and must obtain it from our diet. Deficiency in AsA results in scurvy, since AsA is a critical cofactor in the synthesis of collagen (Murad et al., 1981). Indeed, AsA is a major antioxidant compound involved in many reactions. In mammals, it also plays a role in the protection of DNA from oxidative damage, since AsA eliminates reactive oxygen species (Fraga et al., 1991). In plants, AsA has been suggested to minimize the generation of reactive oxygen species, which alleviates the damage of photosynthetic machinery during photoinactivation (Tóth et al., 2011). In addition, AsA level modulates plant growth and development through altering phytohormone and defense signaling (Pastori et al., 2003). It is known that elevated AsA level confers tolerance to abiotic stresses such as salt and heat stress (Hemavathi et al., 2010; Vacca et al., 2004).

The main synthetic pathway for AsA in vascular plants is Man (sugars in this study are D series unless designated otherwise)/L-galactose pathway (Smirnoff-Wheeler pathway) (Wheeler et al., 1998), in which the conversion of GDP-Man from Man 1-phosphate (Man 1-P) catalyzed by GDP-Man pyrophosphorylase (GMPP) is a rate-limiting step affecting AsA quantity, as well as several downstream steps (Supplemental Figure 1) (Dowdle et al., 2007; Linster et al., 2007; Torabinejad et al., 2009). VITAMIN C DEFECTIVE1 (VTC1)/CYTOKINESIS DEFECTIVE1 (CYT1; hereafter, VTC1 indicates VTC1/CYT1 protein) has been identified as the major form of GMPP in Arabidopsis, and evidence for its key role in AsA synthesis comes from a number of different studies: In *Arabidopsis thaliana*, the *vtc1-1* mutant, a leaky mutant for the *VTC1* gene, exhibits a 70% decrease in AsA level (Conklin et al., 1997, 1999) and a CONSTITUTIVE PHOTOMORPHOGENESIS9 (COP9) signalosome subunit, CSN5B, downregulates AsA level through the degradation of VTC1 in the dark (Wang et al., 2013b). In tomato (*Solanum lycopersicum*), metabolic engineering to increase pyrophosphate (PPi) levels substantially decreased AsA quantity, as it promoted pyrophosphorolysis of GDP-Man into Man 1-P and GTP by GMPP (Osorio et al., 2013). Due to the pivotal role of this enzyme, efforts to enhance AsA levels in planta have targeted *VTC1* gene expression (Cronje et al., 2012). Recently, a transcription factor, ETHYLENE RESPONSE FACTOR98 (ERF98) has been identified as a positive regulator of *VTC1* (Zhang et al., 2012). However, a protein factor that directly stimulates the GMPP activity of VTC1 remains to be identified.

GDP-Man also serves as substrate in the synthesis of the mannan family polysaccharides, which are widely distributed in vascular plants (Scheller and Ulvskov, 2010). These include glucomannan in konjac (*Amorphophallus konjac*; an Asian plant

[1] Address correspondence to kotake@mail.saitama-u.ac.jp.
The author responsible for distribution of materials integral to the findings presented in this article in accordance with the policy described in the Instructions for Authors (www.plantcell.org) is: Toshihisa Kotake (kotake@mail.saitama-u.ac.jp).
www.plantcell.org/cgi/doi/10.1105/tpc.15.00379

containing high levels of glucomannan) and galactomannan in beans (i.e., *Ceratonia siliqua*), which are accumulated as storage polysaccharides and utilized as dietary fibers in our foods. Mannans are also found in gymnosperms such as pine (i.e., *Pinus radiata*) as a major hemicellulose. The synthesis of mannan family polysaccharides is catalyzed by the CELLULOSE SYNTHASE-LIKE As (CSLAs), which form a subclade of CAZy family GT2. In vitro, the CSLAs can transfer mannosyl residues from GDP-Man to produce a homomannan (β-1,4-Man) backbone. However, if GDP-glucose (GDP-Glc) is also provided, a glucomannan backbone is produced (a combination of β-1,4-Man and β-1,4-Glc; Liepman et al., 2005). In Arabidopsis, as shown in the *csla2 csla3 csla9* triple mutant, loss of glucomannan in inflorescence stems has no apparent effect on growth and development (Goubet et al., 2009). However, glucomannan seems to play a specific role in certain cell types, as plants lacking an active CSLA7 are embryo lethal (Goubet et al., 2003). In addition, the *MANNAN SYNTHESIS-RELATED* genes, which encode putative glycosyltransferases with unknown function, have also been shown to be required for glucomannan synthesis (Wang et al., 2013a). Understanding the mechanism for mannan family polysaccharide synthesis would contribute to the improvement of its production. However, the availability of Arabidopsis mutants with defects in glucomannan synthesis is currently limited.

In addition to AsA and mannan polysaccharides, glycoproteins and glycolipids also require GDP-Man for their synthesis. In the early process of *N*-linked glycosylation, GDP-Man is used for the synthesis of the lipid-linked glycan at the cytoplasmic side of the endoplasmic reticulum (ER), which is then translocated via a flippase into the ER lumen, where it is further glycosylated. This is supported by the observation that the *cyt1* mutation, which is allelic to *vtc1*, perturbs the *N*-glycosylation of glycoproteins, resulting in an embryonic lethal phenotype (Lukowitz et al., 2001). Loss of GONST1, a Golgi-localized GDP-sugar transporter, specifically reduced the mannosyl residues of glycosyl inositol phosphorylceramides (GIPCs), causing severe dwarfism without affecting AsA and glucomannan biosynthesis (Mortimer et al., 2013). This suggests that the synthesis of GIPCs requires transport of GDP-Man into the Golgi apparatus by GONST1, but that of AsA and glucomannan do not. A topological study has suggested that CSLAs utilize GDP-Man in the Golgi lumen (Davis et al., 2010), implying the presence of an alternative GDP-Man transporter for glucomannan. Although all of these compounds are independently synthesized, GDP-Man seems to be provided from the identical biosynthesis pathway involving VTC1.

In vascular plants, the majority of nucleotide sugars are found in a GDP- or UDP-linked form, although a few other forms, such as ADP-Glc and CMP-KDO, are also seen. GDP-Man is the starting substrate of the de novo pathway, from which other GDP-sugars, including GDP-L-Fuc and GDP-L-Gal, are formed through interconversion reactions (Reiter and Vanzin, 2001; Reiter, 2008). The physiological importance of GDP-Man as the starting substrate has also been shown. In tomato, the RNAi silencing of a GDP-Man 3,5-epimerase generating GDP-L-Gal in the Man/L-Gal pathway results in the altered structure of the pectin rhamnogalacturonan II, which causes a growth defect (Gilbert et al., 2009; Voxeur et al., 2011). As mentioned above, GDP-Glc likely serves as a donor substrate in the synthesis of glucomannan. While in mammals, GDP-Glc is also synthesized from Glc 1-P by a GMPP complex (Szumilo et al., 1993; Ning and Elbein, 2000), a mechanism for the generation of GDP-Glc remains to be clarified in vascular plants.

Nucleotide sugar pyrophosphorylases are a family of enzymes, many of which catalyze the reversible conversion of nucleotide triphosphate and monosaccharide 1-P to nucleotide diphosphate sugar and PPi. There are at least nine clades of nucleotide sugar pyrophosphorylases (Figure 1A), which have different activities and physiological functions (Kotake et al., 2010). UDP-Glc pyrophosphorylases generate UDP-Glc, the starting substrate of UDP-sugar metabolism, which is used for the synthesis of cellulose and β-1,3-glucan and for the β-1,4-glucan backbone of xyloglucan (Hayashi et al., 1987; Gordon and Maclachlan, 1989; Cocuron et al., 2007; Park et al., 2010). A plant-specific enzyme, UDP-sugar pyrophosphorylase (USP), converts various monosaccharide 1-Ps to their respective UDP-sugars in the salvage pathway and is required for pollen development (Kotake et al., 2004, 2007; Schnurr et al., 2006). ADP-Glc pyrophosphorylases provide ADP-Glc for starch synthesis and can be divided into two clades, small (S) subunit and large (L) subunit clades. As reported for ADP-Glc pyrophosphorylase S1 of Arabidopsis, the S subunit plays a central role in the synthesis of ADP-Glc, whereas the L subunit has weak enzymatic activity and instead functions as regulatory protein to enhance the activity of the S subunits (Crevillén et al., 2003; Petreikov et al., 2010).

In this study, proteins structurally resembling nucleotide sugar pyrophosphorylases were identified as key factors for the generation of GDP-Man in Arabidopsis. The mutants lacking these proteins showed a drastic reduction in GMPP activity as well as significantly lowered AsA level and glucomannan accumulation in cell walls. Based on the analysis of decreased GMPP activity in the mutants, properties of recombinant proteins, and interaction with VTC1, we suggest that these proteins participate in the synthesis of GDP-Man through stimulation of the GMPP activity of VTC1.

RESULTS

Drastic Decrease in GMPP Activity in *konjac* Mutants

Based on a phylogenetic analysis of nucleotide sugar pyrophosphorylases from Arabidopsis and rice (*Oryza sativa*), two proteins, designated KONJAC1 (KJC1) and KJC2, were found to belong to a clade close to the GMPP clade (Figure 1A; Supplemental File 1). Although KJCs show weak sequence similarity to VTC1 (identities of KJC1 and KJC2 to VTC1, 31 and 32%, respectively; Supplemental Figure 2) that plays a central role in the synthesis of GDP-Man, they have an insertion of two amino acids in the pyrophosphorylase consensus motif that is highly conserved in GMPPs (Figure 1B). These observations suggest that KJCs are involved in GDP-sugar metabolism but may have a function different from VTC1.

To explore the functions of KJCs, the homozygous T-DNA insertion lines *kjc1-1* (SALK_044963) and *kjc2-1* (SALK_023876) and the double mutant *kjc1-1 kjc2-1* were characterized (Supplemental Figure 3A). Their genotypes were confirmed by RT-PCR (Supplemental Figure 3B and Supplemental Table 1).

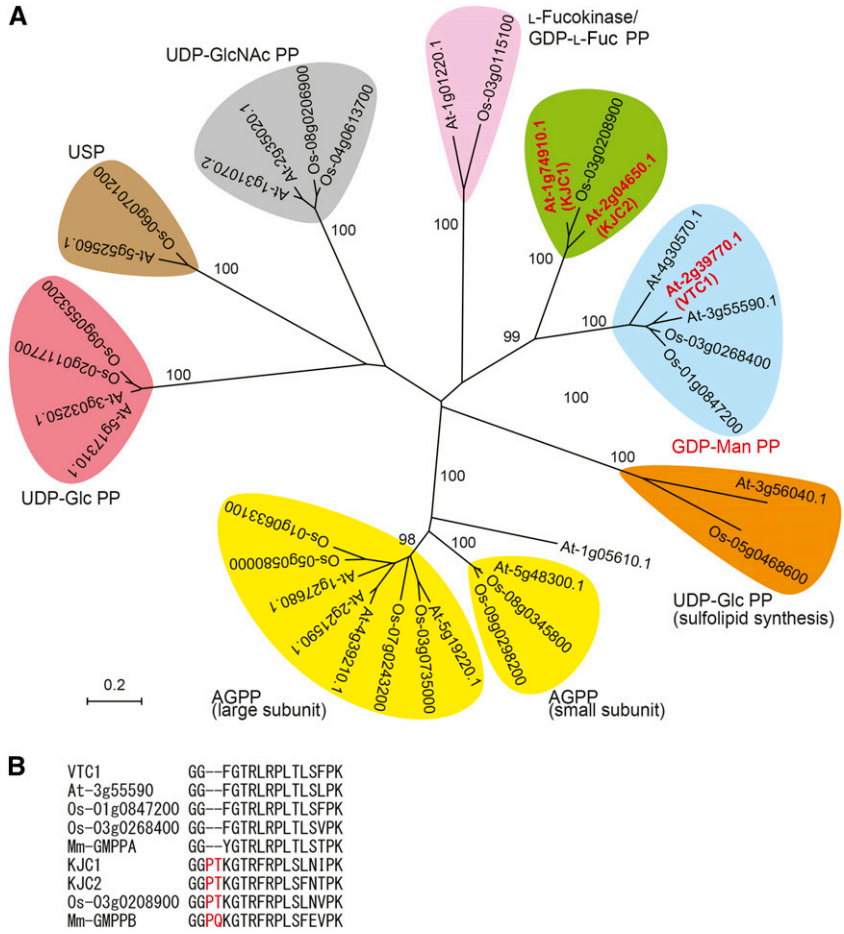

B

VTC1	GG--FGTRLRPLTLSFPK
At-3g55590	GG--FGTRLRPLTLSLPK
Os-01g0847200	GG--FGTRLRPLTLSFPK
Os-03g0268400	GG--FGTRLRPLTLSVPK
Mm-GMPPA	GG--YGTRLRPLTLSTPK
KJC1	GGPTKGTRFRPLSLNIPK
KJC2	GGPTKGTRFRPLSFNTPK
Os-03g0208900	GGPTKGTRFRPLSLNVPK
Mm-GMPPB	GGPQKGTRFRPLSFEVPK

Figure 1. Relationships of KJCs with Other Nucleotide Sugar Pyrophosphorylases.

(A) The phylogenetic relationships of KJC1 and KJC2 with other nucleotide sugar pyrophosphorylases in Arabidopsis and rice. The analysis was performed using MEGA software (version 6.0; Tamura et al., 2013). The bar indicates substitutions per site. PP, pyrophosphorylase. Numbers in nodes represent bootstrap values.

(B) The pyrophosphorylase consensus motifs of VTC1 and KJCs. The insertion of two amino acids observed for the KJC subfamily is shown in red. Mm-GMPPA and Mm-GMPPB, mouse (*Mus musculus*) GDP-Man pyrophosphorylase subunits α and β, respectively.

First, soluble GMPP activity of the mutants was measured using Man 1-P and GTP as the substrates. Surprisingly, the activities in *kjc1-1* and *kjc1-1 kjc2-1* double mutants were only 10 and 8% of the wild type, respectively, based on the protein content (Figure 2). Similar results were obtained for GMPP activity based on the fresh weight (Supplemental Figure 4). GMPP activity in *kjc1-1* was properly recovered by the complementation with a genomic *KJC1* fragment (Supplemental Figure 5). In addition, a second *kjc1* mutant, *kjc1-2* (SALK_110173), in which T-DNA is inserted at the end of coding region was isolated, showed a 19% reduction in GMPP activity. These results suggest that KJC1 participates in the synthesis of GDP-Man as a key factor affecting GMPP activity. On the other hand, there was no significant reduction in the activity in *kjc1-3*, a T-DNA insertion line (GK_175D06) that has a T-DNA insertion in 5′ upstream region (Supplemental Figure 3A). The activity in the *kjc2-1* mutant was ~70% of the wild type. The large reduction in GMPP activity in the *kjc1-1* and *kjc1-1 kjc2-1* mutants was unexpected, since the *kjc* mutants contain wild-type VTC1 protein. This suggests that KJC proteins can modulate the GMPP activity of VTC1, as opposed to functioning as additional GMPPs. The results also indicate that KJC1 and KJC2 can be considered as the major and minor isoforms, respectively, consistent with their expression levels obtained from publicly available microarray data (Hruz et al., 2008; Supplemental Figure 6A).

AsA Levels in *kjc* Mutants

GDP-Man synthesis is one of the rate-limiting steps in AsA synthesis, as shown in plants with reduced amounts of functional VTC1 (Conklin et al., 1997). Therefore, the influence of *kjc* mutations on AsA level in seedlings was also investigated. Consistent with reduced GMPP activity, AsA levels (here, total AsA levels were measured) in *kjc1-1* and *kjc1-1 kjc2-1* were ~40% of that in the wild-type plant, while the reduction was smaller in *kjc2-1* (Figure 3). AsA level in *kjc1* was comparable with that in *vtc1*

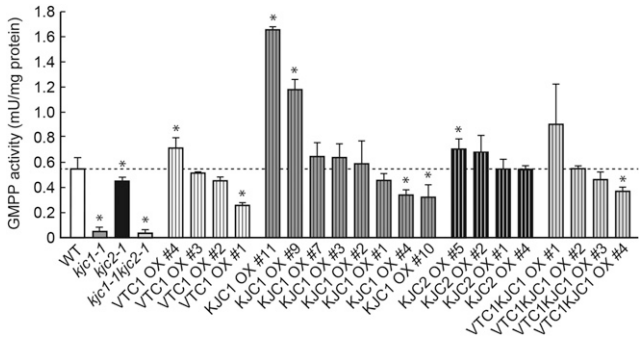

Figure 2. GMPP Activity in *kjc* Mutants and *KJC*-Overexpressing Plants.

The activity was assayed in 2-week-old seedlings of the wild type, *kjc1-1*, *kjc2-1*, and *kjc1- 1kjc2-1* mutants and those overexpressing *VTC1* (VTC1 OX), *KJC1* (KJC1 OX), *KJC2* (KJC2 OX), and both *KJC1* and *VTC1* (VTC1KJC1 OX) using Man 1-P and GTP as the substrates. Data are mean values with SD ($n = 3$ biological replicates). The asterisk indicates significant difference from the wild type (Student's *t* test, $P < 0.05$). In this figure, GMPP activity per milligram protein is shown, and that per gram fresh weight is shown in Supplemental Figure 4.

(25% of the wild-type plant) (Conklin et al., 1999), although the results cannot be directly compared, as growth conditions were not necessarily the same. Thus, KJC proteins can be defined as a factor affecting the synthesis of AsA.

KJC1 Affects GMPP Activity

The effect of overexpression of *KJC1* and *KJC2* genes on GMPP activity was also examined. In several independently generated lines overexpressing either *KJC1* or *KJC2* under the control of the CaMV 35S promoter (Supplemental Figure 7A), significant increases in GMPP activity were observed (Figure 2), while the expression level of *VTC1* was not increased (Supplemental Figures 7A and 7B). Moreover, overexpression of *KJC1* also caused a maximum of 37% increase in AsA level (Figure 3). These results strongly support the hypothesis that KJCs participate in the generation of GDP-Man. Although overexpression of *VTC1* was also examined, the effects on GMPP activity and AsA level were not obvious compared with that of *KJC1* (Figures 2 and 3). Therefore, the turnover of VTC1 might be regulated by other factors (Wang et al., 2013b).

Reduced GDP-Man Level in *kjc1-1* Mutant

It is highly probable that GMPP activity determines the level of GDP-Man. The influence of *kjc* mutations on the metabolism and accumulation of GDP-Man was analyzed. Nucleotide sugars including GDP-Man were extracted from liquid-grown calli of *kjc* and *vtc* mutants, separated, and quantified by liquid chromatography-mass spectrometry/mass spectrometry (LC-MS/MS). Consistent with decreased GMPP activity, out of the 10 NDP-sugars measured, only GDP-Man level was significantly reduced in the *kjc1-1* mutant (Figure 4). While the level of GDP-Man in *vtc2-1*, which has a defect in the conversion of GDP-L-Gal to L-Gal 1-P, was similar to that in the wild type, *vtc1-1* showed a more drastic reduction than *kjc1-1*. The level of GDP-Glc was quite low in all plants and was not significantly different between the mutants and the wild type. The decreased level of GDP-Man in *kjc1-1* strongly supports the hypothesis that KJC1 affects the activity of VTC1, a major isoform of GMPP in Arabidopsis.

The Role of KJC Proteins in Growth and Development

The growth of *kjc* mutants was examined. While *kjc1-1* and *kjc2-1* single mutants grew normally, *kjc1-1 kjc2-1* exhibited severe dwarfism (Figures 5A and 5B). The double mutant had small leaves and short roots and did not flower. These phenotypes indicate that KJC proteins are important for normal growth and development. The expression data available from the Arabidopsis eFP browser indicate that the expression of *KJC1* is under diel regulation; thus, its level is high in the dark (Supplemental Figure 6B; Winter et al., 2007). KJC1 protein may participate in the regulation of AsA level.

In the *cyt1* mutant (which is allelic to *vtc1*), an embryonic lethal phenotype caused by *N*-linked glycosylation deficiency was observed (Lukowitz et al., 2001). Although KJCs participate in the synthesis of GDP-Man together with VTC1, a significant increase in impaired seeds was not observed for *kjc1-1* and *kjc2-1* single mutants (Supplemental Figure 8). Thus, the physiological importance of KJC proteins is not necessarily identical to that of VTC1.

Amount and Structure of Cell Wall Glucomannan

GDP-Man is utilized as a direct substrate in the synthesis of cell wall glucomannan. It is highly probable that, together with CSLA activity, the available pool of GDP-Man determines the accumulation and structure of glucomannan in cell walls. To examine changes in cell wall glucomannan in the *kjc* mutants, the sugar composition of cell walls in the seedlings was determined. The proportion of Man constituting cell wall polysaccharides in *kjc1-1*

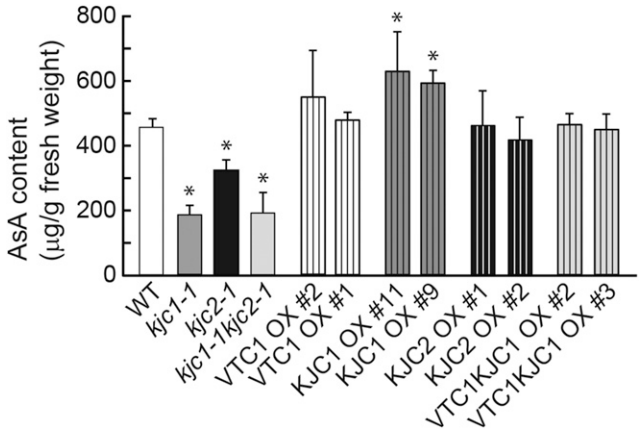

Figure 3. AsA Level in *kjc* Mutants and *KJC*-Overexpressing Plants.

Total AsA level was measured in 2-week-old seedlings of the wild type, *kjc1-1*, *kjc2-1*, and *kjc1-1 kjc2-1* mutants and those overexpressing *VTC1* (VTC1 OX), *KJC1* (KJC1 OX), *KJC2* (KJC2 OX), and both *KJC1* and *VTC1* (VTC1KJC1 OX). Data are mean values with SD ($n = 3$ biological replicates). The asterisk indicates significant difference from the wild-type plant (Student's *t* test, $P < 0.05$).

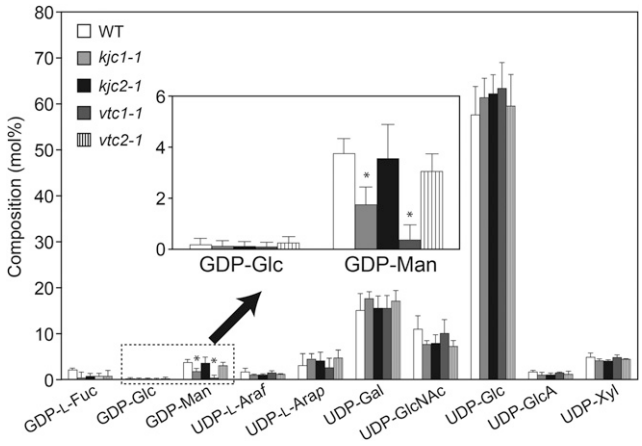

Figure 4. Level of GDP-Man in *kjc* and *vtc* Mutants.

Nucleotide sugars were extracted from liquid-grown calli of *kjc* and *vtc* mutants and analyzed by LC-MS/MS. Data are mean values with SD ($n = 3$ biological replicates). The asterisk indicates significant difference from the wild-type plant (Student's *t* test, $P < 0.05$).

and *kjc1-1 kjc2-1* was ~50% of the wild type (Figure 6A). As almost all Man detected in cell wall preparations in Arabidopsis is glucomannan derived (Goubet et al., 2009), this result indicates that these mutants have reduced levels of glucomannan in their cell walls. To confirm the changes in cell wall glucomannan, polysaccharide analysis using carbohydrate gel electrophoresis (PACE) was also performed (Goubet et al., 2002, 2009). Here, cell wall (AIR, for alcohol-insoluble residue) was prepared from seedlings and hydrolyzed by a combination of β-1,4-mannanases. The resulting oligosaccharides were then labeled with a fluorescent tag and separated by gel electrophoresis. As shown in Figure 6B, the quantity of mannanase-dependent oligosaccharide bands in *kjc1-1* and *kjc1-1 kjc2-1* was lower than those in the wild-type plant (based on the band intensity, estimated glucomannan contents in *kjc1*-1 and *kjc1-1 kjc2-1* were 64% ± 12% and 79% ± 9% of the wild type, respectively). By comparison, when *KJC1* was overexpressed, more glucomannan was detected (KJC OX # 9 and 11, 158% ± 40% and 123% ± 21% of the wild type, respectively).

N-Glycan Structure in *kjc* Mutants

In the *cyt1* mutant, the deficiency in GDP-Man affects the *N*-glycosylation of glycoproteins (Lukowitz et al., 2001). In vascular plants, the glycan core is substituted with a β-1,2-xylosyl residue attached to a mannosyl residue and with an α-1,3-L-fucosyl residue attached to the reducing terminal *N*-acetylglucosaminosyl residue (Supplemental Figure 9A). Protein gel blot analyses of the seedlings of *kjc* mutants were performed using antibodies against these glycosyl residues (Faye et al., 1993). Although a change in the band pattern (increase in an unidentified protein with relative molecular mass of 24 kD) was observed in *kjc1-1 kjc2-1* mutant, proper β-1,2-xylosyl and α-1,3-L-fucosyl residues of *N*-glycans were observed for *kjc1-1*, *kjc2-1*, and *kjc1-1 kjc2-1* mutants (Supplemental Figures 9B and 9C). These results suggest that the core structure of *N*-glycans is not altered in *kjc* mutants.

Mannosylation of GIPCs in *kjc* Mutants

In vascular plants, GIPCs generally have inositol, glucuronic acid, *N*-acetylglucosamine, and Man as their headgroup sugars, depending on species and tissue type. In the *gonst1* GDP-sugar transporter mutant, reduced mannosylation of GIPC occurs, which causes dwarfism and a constitutive hypersensitive response (Mortimer et al., 2013). To examine the influence of *kjc* mutations on GIPC mannosylation, the sugar composition of GIPCs in calli of *kjc* mutants was determined by LC-MS/MS analysis. Although the proportion of GIPCs having two hexoses was slightly reduced in *kjc1-1* and *kjc2-1* mutants (Supplemental Figure 10), the change was minor in comparison with the *gonst1* mutant, in which more than 70% of GIPCs lacked headgroup sugar (Mortimer et al., 2013).

Properties of Recombinant KJC1 and 2

To gain an insight into the molecular functions of KJC proteins, recombinant KJC1 (rKJC1) and KJC2 (rKJC2) were prepared by heterologous expression in *Escherichia coli* together with recombinant VTC1 (rVTC1). The recombinant proteins were expressed as proteins fused to His_6 tags and purified by chelating chromatography (Supplemental Figure 11A). While rVTC1 showed proper GMPP activity, forming GDP-Man from Man 1-P and GTP,

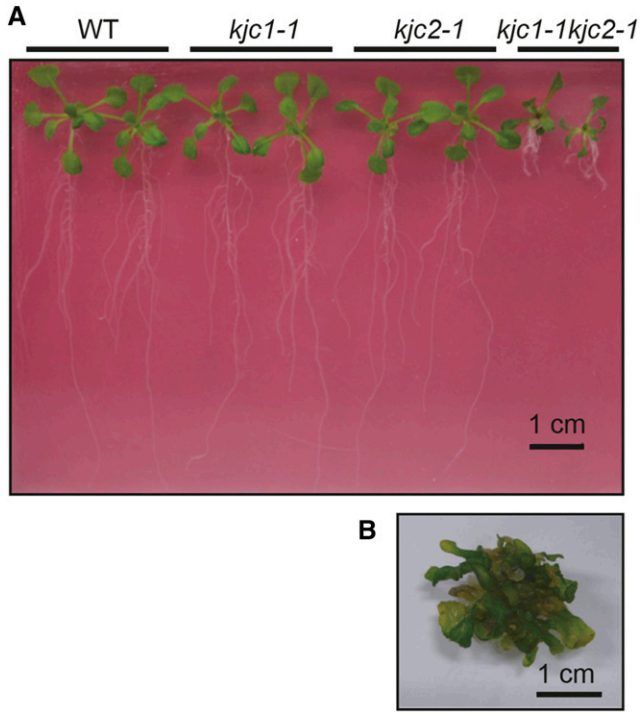

Figure 5. KJC Proteins Are Important for Growth and Development.

(A) Severe dwarfism of *kjc1-1 kjc2-1* mutant. Significant differences in growth were not observed for *kjc1-1* and *kjc2-1*. The plants were germinated and grown on vertical MS-agar plates under continuous light for 2 weeks.

(B) *kjc1-1 kjc2-1* mutant grown on MS-agar plate for 5 weeks. The double mutant did not develop an inflorescence stem.

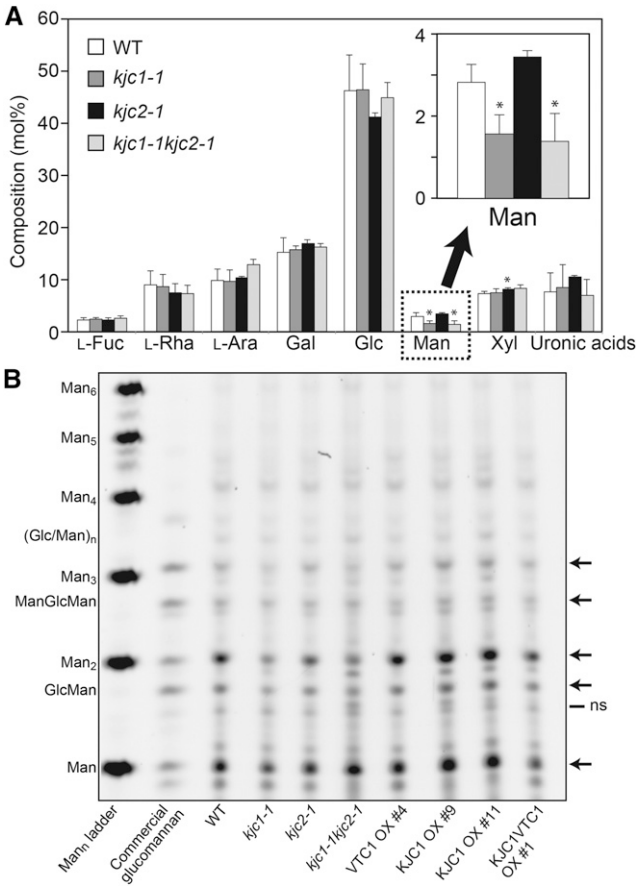

Figure 6. Cell Wall Composition of *kjc* Mutants and *KJC*-Overexpressing Plants.

(A) Monosaccharide composition of the *kjc* cell wall. *kjc* mutant seedling cell walls were fractionated and hydrolyzed by sulfuric acid, and the monosaccharide composition was determined by high-performance anion-exchange chromatography with pulsed amperometric detection. A combined value from the insoluble and soluble fraction is shown for each monosaccharide. Data are mean values with SD (n = 3 biological replicates). The asterisk indicates significant difference from the wild-type plant (Student's t test, $P < 0.05$).

(B) PACE of mannan polysaccharides in the cell wall of seedlings of *kjc* mutants and *KJC*-overexpressing plants. Glucomannan oligosaccharides released from 2-week-old seedling AIR hydrolyzed with β-1,4-mannanases were derivatized using 2-aminonaphthalene trisulfone, and then separated by polyacrylamide gel electrophoresis. The oligosaccharides prepared from commercial glucomannan were used as standards. Arrows indicate Man and oligosaccharides derived from mannan polysaccharide, and ns indicates a nonspecific band from a compound in the reaction reagents. A representative gel is shown, and the experiment was performed on three biological replicates, each with two technical replicates.

rKJCs showed neither GMPP activity (Figure 7A), GDP-Glc pyrophosphorylase (GGPP) activity, nor GDP-L-Fuc pyrophosphorylase activity. However, higher GMPP activity than rVTC1 alone was observed when rVTC1 was mixed with rKJC1 or rKJC2 at molar ratio of 1:1 (Figure 7B). This raised two possibilities: rKJCs stimulated the activity of rVTC1 or rKJCs gained GMPP activity by interacting with rVTC1. To examine these possibilities, rKJCs and rVTC1 with a point mutation in the highly conserved nucleotide sugar pyrophosphorylase consensus motif, rVTC1 K23A, rKJC1 K33A, and rKJC2 K30A, were prepared (Supplemental Figure 11B) (Kotake et al., 2008). While rVTC1 K23A did not show any activity even in the presence of rKJCs, high activity was observed for mixtures of normal rVTC1 and rKJC1 K33A, and normal rVTC1 and rKJC2 K30A (Figure 7B). These results show that KJC proteins stimulate the activity of rVTC1.

In pig liver, GMPP exists as a complex of subunits α and β, which, based on the similarity of their amino acid sequences, correspond to KJCs and VTC1, respectively (Figure 1B; Supplemental Figure 12 and Supplemental File 2). Importantly, besides GMPP activity, the animal GMPP complex has high GGPP activity, while subunit β alone had very weak GGPP activity (Szumilo et al., 1993; Ning and Elbein, 2000). In this context, substrate specificity of the mixture of rVTC1 and rKJCs was compared with that of rVTC1 alone using various nucleotide sugars and PPi as the substrates. However, obvious changes in the substrate specificity were not observed, when the activity toward GDP-Man (GDP-Man pyrophospholysis activity) with or without rKJCs is taken as 100% (Supplemental Table 2). Indeed, GGPP activity in seedlings (<5% of the detected GMPP activity) and the level of GDP-Glc in the callus (4.5% of GDP-Man) was low even in the wild type, indicating that the complex of KJC1 and VTC1 does not have high GGPP activity.

Interaction of KJC Proteins with VTC1

The drastic reduction of GMPP activity in *kjc1-1* and *kjc1-1 kjc2-1* suggested that KJC1 forms a complex with VTC1 and affects its GMPP activity. The interaction of KJC1 and KJC2 with VTC1 was examined by yeast two-hybrid (Y2H) assay. As shown in Figures 8A and 8B, KJC1 and KJC2 appeared to interact with VTC1 in yeast cells, while it did not interact with USP, which catalyzes the formation of UDP-sugars (Supplemental Figure 13). In addition, the Y2H assay also suggested the formation of homo- and heterodimers of KJC proteins, whereas VTC1 does not likely form a homodimer.

The interaction between KJC1 and VTC1 was also confirmed by a copurification assay of the recombinant proteins. We examined whether rFLAG-KJC1 is retained by the Ni-chelating column via interaction with $rHis_6$-VTC1. As shown in Figure 8C, a proportion of the rFLAG-KJC1 was retained and coeluted with $rHis_6$-VTC1 with imidazole solution, while rFLAG-KJC1 alone was hardly retained on the column (Figure 8D). These results indicate that KJC proteins form a complex with VTC1, suggesting that they may thereby influence the GMPP activity of VTC1.

DISCUSSION

KJCs Stimulate GMPP Activity of VTC1

Generation of GDP-Man relies only on GMPP activity, whereas UDP-Glc, the starting substrate in the de novo pathway of UDP-sugars, can be formed by different enzymes: UDP-Glc pyrophosphorylase, USP, or sucrose synthase (Kotake et al., 2004). Out of three GMPP isoforms in Arabidopsis, VTC1 is the main isoform based on the expression level and its mutant phenotypes (Conklin et al., 1999;

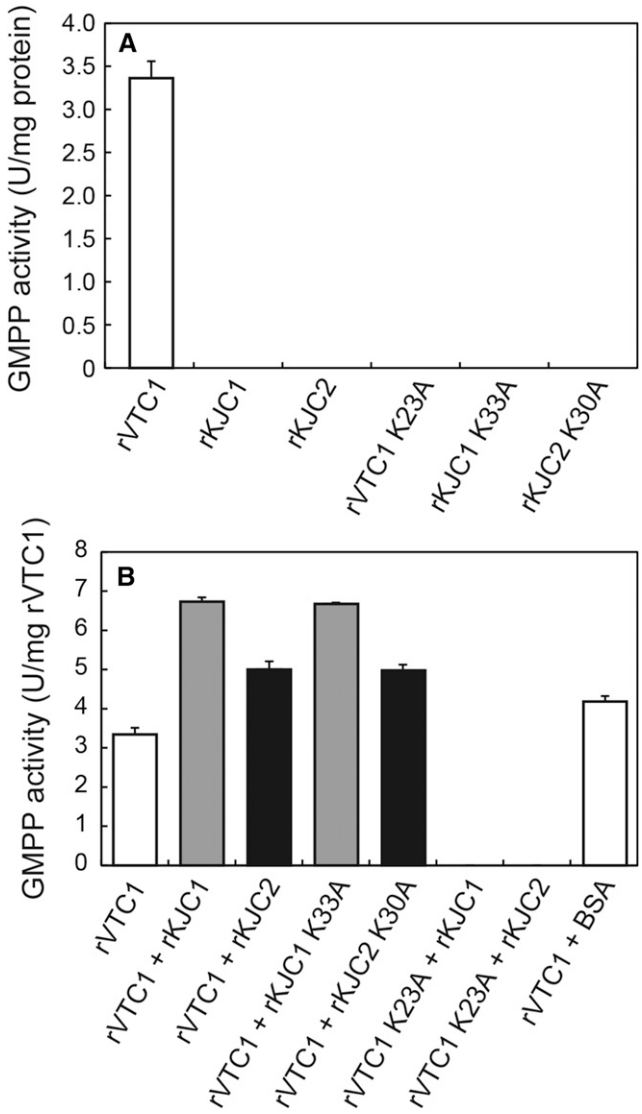

Figure 7. Effect of rKJCs on GMPP Activity of rVTC1.

(A) The rVTC1, rKJC2, rKJC2, and the point-mutated proteins (rVTC1 K23A, rKJC1 K33A, and rKJC2 K30A) were expressed in *E. coli*, and their GMPP activity was examined.

(B) The effect of rKJCs on GMPP activity of rVTC1. The rKJC protein was added to the reaction mixture at identical concentration to that of rVTC1. The activities per milligram of rVTC1 protein were compared. The rKJCs had no GMPP activity, but they enhanced the activity of rVTC1. The rKJCs with a point mutation also worked on rVTC1. The experiment was performed with three technical replicates. The positions of point-mutated amino acid residues are shown in Supplemental Figure 11B.

Lukowitz et al., 2001). Therefore, the level of GDP-Man is expected to be determined primarily by the activity of VTC1. In this study, on the basis of the results on *kjc* mutants, overexpression of *KJCs*, and recombinant KJCs, KJC1 and KJC2, were identified as factors stimulating GMPP activity of VTC1. The drastic decrease in GMPP activity in the *kjc1-1* mutant indicates that KJC1 is a key factor for the synthesis of GDP-Man in conjunction with VTC1 in Arabidopsis, while KJC2 likely functions as the minor isoform, in specific tissues, or with other GMPP isoforms.

Molecular Functions of KJCs

Based on the properties of recombinant proteins and interaction with VTC1, KJCs were revealed to have neither GMPP nor GGPP activity, but KJCs stimulates the GMPP activity of VTC1, probably through the formation of a complex. Proteins corresponding to KJCs are widely distributed in eukaryotes including mammals (Supplemental Figure 12), but this does not imply conserved functionality. A native GMPP was purified from pig liver comprising a complex of subunits α and β, which correspond to KJC1 and VTC1, respectively (Szumilo et al., 1993; Ning and Elbein, 2000). Importantly, the native complex had GGPP activity higher than GMPP activity, but recombinant subunit β expressed in *E. coli* showed high GMPP activity and very low GGPP activity. This finding suggests that the subunit α has GGPP activity or confers the activity to the complex (Ning and Elbein, 2000). In this work, consistent with its activities in Arabidopsis seedlings, rVTC1 showed relatively low GGPP activity compared with its GMPP activity, even in the presence of rKJC1. We cannot exclude the possibility that the properties of rKJCs expressed in *E. coli* do not properly reflect those of native KJCs, but our results suggest that KJCs themselves do not or rarely synthesize GDP-Man but participate in the generation of GDP-Man through the stimulation and/or stabilization of VTC1.

Recently, another function of the subunit α has also been described. On the basis of strongly increased level of GDP-Man in the lymphoblasts of individuals with a homozygous mutation in the subunit α gene, the subunit α is presumed to mediate a feedback inhibition of subunit β as a regulatory subunit (Koehler et al., 2013). The molecular function of KJCs is similar to that of the mammalian subunit α in the sense that they work as regulatory subunits, but the effect on GMPP activity of the catalytic GMPP is rather opposite to that of mammalian subunit α. Thus, it is suggested that the mammalian subunit α and KJCs share a common ancestor but have acquired different functions (Supplemental Figure 12).

Based on the expression data from Arabidopsis eFP browser, the expression of *KJC1* is high in the dark (Supplemental Figure 6B; Winter et al., 2007; Michael et al., 2008). As the generation of GDP-Man is regulated through degradation of VTC1 by a COP9 signalosome in the dark (Wang et al., 2013b), it is likely that KJC1 also participates in this regulation. KJC1 likely has a function opposite that of the COP9 signalosome in the generation of GDP-Man.

The dramatic decrease in GMPP activity in *kjc1-1* also suggests another function for KJC proteins. In vivo, the absence of KJC1 resulted in a 90% reduction in GMPP activity. In vitro, rKJC1 was only able to boost the GMPP activity of rVTC1 2-fold. This could be due to the nature of the in vitro assay versus in vivo conditions. However, it could also be due to a role for KJC in stabilizing VTC1 in Arabidopsis.

Generation of GDP-Glc by VTC1 and KJC1

GDP-Glc has been shown to serve as the substrate for recombinant CSLA expressed in insect cells in vitro (Liepman et al., 2005). The relatively low GGPP activity of rVTC1, even in the presence of

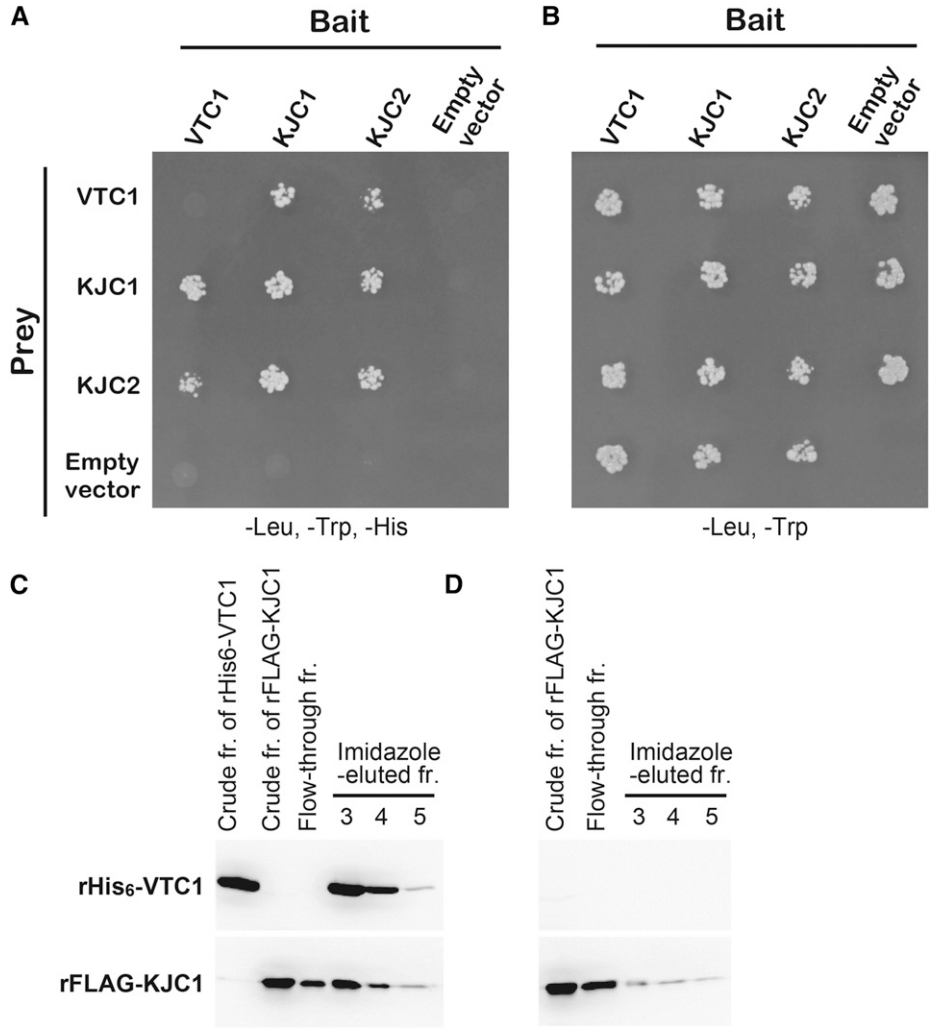

Figure 8. Interaction of KJCs with VTC1.

(A) Interaction between KJC1, KJC2, and VTC1 in yeast cells. The yeast strain, Y2H gold, transformed with a bait plasmid and a prey plasmid was grown on SD medium without His, Leu, and Trp. As negative controls, empty bait and prey plasmids were used. Specific interaction was also confirmed using UDP-sugar pyrophosphorylase as the negative control, as shown in Supplemental Figure 13.

(B) The transformation of the yeast was confirmed on SD medium without Leu and Trp. A representative result is shown, and the experiment was performed with three technical replicates.

(C) Copurification assay for rFLAG-KJC1 and rHis6-VTC1 was performed. A mixture of rFLAG-KJC1 and rHis6-VTC1 was applied to a Ni-chelating column. With 250 mM imidazole, some rFLAG-KJC1 was coeluted with rHis6-VTC1 that bound to Ni-chelating column. The presence of rFLAG-KJC1 and rHis6-VTC1 in the flow-through fraction and eluted fractions was detected by protein gel blot analysis. Crude fractions of rFLAG-KJC1 and rHis6-VTC1 were used as positive controls.

(D) The rFLAG-KJC1 alone was applied to the column. fr, fraction. A representative result is shown, and the experiment was performed with two technical replicates.

rKJC1, raises the question of how GDP-Glc is generated in intact plants. Recent biochemical studies of the GDP-L-Gal phosphorylases, VTC2 and VTC5, have indicated that GDP-Glc can be formed from Glc 1-P and GDP-L-Gal, but this GDP-Glc synthesis pathway is dependent on the synthesis of GDP-L-Gal via GDP-Man (Linster et al., 2007; Wolucka and Van Montagu, 2007). On the other hand, it is also possible that VTC1 generates GDP-Glc from Glc 1-P and GTP in the presence of relatively high concentrations of Glc 1-P in vivo. In this case, the KJCs also likely participate in the synthesis of GDP-Glc with VTC1.

Different Effects of Mutation on AsA, Glucomannan, and *N*-Glycan

The *kjc1-1* mutation appeared to significantly reduce AsA level and glucomannan content, but it did not drastically affect α-L-fucosyl and β-xylosyl residues of *N*-glycans, at least as detected by the immunoblotting method used in this study. Mannosylation of glycoproteins occurs via the dolichol (Dol) import pathway in the ER. In this pathway, GDP-Man is the substrate at the cytosolic face of the ER for mannosylation of a $GlcNAc_2$-PP-Dol intermediate.

The sugars are then translocated across the ER membrane via a flippase, where it is further glycosylated prior to transfer onto the protein. Therefore, it is possible that the different influences on these compounds may result from distinct subcellular localization or different affinities of the enzymes catalyzing these reactions, leading to different priorities for the utilization of GDP-Man as the substrate to a certain reaction. Different impacts on AsA and glucomannan quantities were also observed as a result of overexpression of *KJC1*. While the overexpression slightly increased AsA level, it caused significant increase in glucomannan content in cell walls. It is likely that control mechanisms exist to limit excess AsA levels in order to maintain the redox balance in the cells.

Dwarfism of the *kjc1-1 kjc2-1* Mutant

Severe dwarfism was observed for the *kjc1-1 kjc2-1* mutant, while its AsA concentration and glucomannan cell wall content were comparable to those of *kjc1-1*. The phenotypes of *kjc1-1 kjc2-1* are not necessarily consistent with those of other mutants with defects in AsA and glucomannan synthesis, including *cyt1* and *csla* mutants. First, *kjc1-1 kjc2-1* was viable, which is distinct from the embryonic lethal phenotype of *cyt1* (*N*-glycosylation) and *csla7* (glucomannan) mutants (Lukowitz et al., 2001; Goubet et al., 2003). Second, there was no evidence of any constitutive cell death, as seen when mannosylation of GIPCs is defective (Mortimer et al., 2013). Third, there was no detectable defect in *N*-glycosylation, which resulted in perturbed cellulose synthesis in *cyt1* (Lukowitz et al., 2001). In this study, a clear explanation for the dwarfism phenotype was not obtained, but it is likely that an unknown metabolite also requires relatively high concentrations of GDP-Man. It is also possible that a specific cell type uses KJCs to boost GDP-Man metabolism.

Future Interests

KJCs appear to be key regulatory factors in GDP-Man generation by VTC1. The activity of VTC1 is also regulated by other factors, such as the COP9 signalosome CSN5B and transcription factor ERF98. A concerted mechanism likely exists for the regulation of VTC1 activity by environmental stress/signals, such as light, in vascular plants. It would be important to clarify how KJCs participate in this concerted mechanism.

METHODS

Plant Material

Arabidopsis thaliana ecotype Col was used in this study. The T-DNA insertion lines SALK_044963, SALK_110173, GK_175D06, and SALK_023876 (genetic background, Col) provided by the Nottingham Arabidopsis Stock Center were used as *kjc1-1*, *kjc1-2*, *kjc1-3*, and *kjc2-1*, respectively. The double mutant, *kjc1-1 kjc2-1*, was generated by a cross between *kjc1-1* and *kjc2-1*. The *vtc1-1* and *vtc2-1* mutants were provided by N. Smirnoff of Exeter University. For the measurement of AsA level, GMPP activity, and glucomannan amount, seedlings were germinated and grown on Murashige and Skoog (MS) medium in 0.8% (w/v) agar under continuous light (cold cathode fluorescent lamp; Biomedical Science) at 23°C for 2 weeks. The genotypes of the mutants were determined using specific primers (Supplemental Figure 3A and Supplemental Table 1).

For the construction for overexpression of *KJC1*, *KJC2*, and *VTC1*, each cDNA was amplified with a set of specific primers shown in Supplemental Table 1 and cloned between the *Bam*HI site and *Sac*I site of the binary vector pBI121 (Clontech) to be expressed under the control of the CaMV 35S promoter. The plasmid construct was introduced into Arabidopsis (ecotype Col) by an Agrobacterium-mediated (*Rhizobium radiobacter*, EHA105 strain) method (Clough and Bent, 1998).

Complementation of the *kjc1-1* Mutant

A genomic fragment of the *KJC1* gene (4 kb) including 0.8 kb of upstream sequence was amplified with primers, gKJC1-EcoRI-F and gKJC1-HindIII-R (Supplemental Table 1). The DNA fragment was digested with *Eco*RI and *Hin*dIII and subcloned into the binary vector pBGGN (Inplanta Innovation) to yield the construct gKJC1/pBGGN. The construct was introduced into *kjc1-1* mutant by an Agrobacterium-mediated (*R. radiobacter*, EHA105 strain) method.

Measurement of GMPP Activity in Plants

Arabidopsis seedlings were homogenized with a mortar and pestle in homogenization buffer A containing 50 mM Tris-HCl buffer, pH 8.0, 20% (w/v) glycerol, and 1 mM PMSF. The homogenate was centrifuged at 8000*g* for 5 min to remove cell debris (Kotake et al., 2004) and then used as a crude enzyme fraction. The activity of GMPP was determined by monitoring the formation of GDP-Man. The reaction mixture contained 50 mM 3-morpholinopropanesulfonic acid-KOH buffer, pH 7.0, 2 mM $MgCl_2$, 10 mM GTP, and 1 mM Man 1-P. The reaction products were detected and quantified with an HPLC system using a Shimadzu LC-10AD equipped with a CarboPac PA1 column (4 × 250 mm; Dionex) according to the method described by Pauly et al. (2000). GDP-Man, GDP-Glc, GTP, Glc-1-P, and Man-1-P were purchased from Sigma-Aldrich.

RT-PCR

Total RNA was extracted from 2-week-old seedlings of *kjc* mutants and *KJC*-overexpressing plants with an RNeasy Plant Mini kit (Qiagen) according to the manufacturer's instructions. Single-stranded cDNA was synthesized using the reverse transcriptase ReverTra Ace-α- (Toyobo) and an oligo$(dT)_{12-18}$ primer.

For the amplification of full-length coding sequences (CDSs) for *KJC1*, *KJC2*, and *VTC1*, primer sets KJC1-full-F and KJC1-full-R for *KJC1*, KJC2-full-F and KJC2-full-R for *KJC2*, VTC1-full-F and VTC1-full-R for *VTC1* (Supplemental Table 1) were designed based on the genomic database of Arabidopsis (TAIR; www.arabidopsis.org). The PCR was performed with a Mighty Amp polymerase kit (Takara Bio).

For the quantitative RT-PCR, the primer sets ACT2-Q-RT-PCR-F and ACT2-Q-RT-PCR-R for *ACTIN2*, KJC1-Q-RT-PCR-F and KJC1-Q-RT-PCR-R for *KJC1*, KJC2-Q-RT-PCR-F and KJC2-Q-RT-PCR-R for *KJC2*, and VTC1-Q-RTPCR-F and VTC1-Q-RT-PCR-R for *VTC1* (Supplemental Table 1), were designed using the Primer 3.0 program (Untergasser et al., 2012). The PCR was performed with a SYBR Premix ExTaq kit (Takara Bio). The experiment was performed on three biological replicates, each with two technical replicates.

Preparation and Characterization of Recombinant Enzymes

The CDSs of *KJC1*, *KJC2*, and *VTC1* amplified with sets of specific primers (Supplemental Table 1) were subcloned between the *Nde*I site and *Bam*HI site of pET15b expression vector (Novagen), which was designed to express the recombinant enzyme fused to His_6 tags at the N terminus. Point mutation was introduced into *KJC* cDNAs by PCR using specific sets of primers (Supplemental Table 1). Point mutation was also introduced into

VTC1 cDNA with PrimeStar Mutagenesis Basal kit (Takara Bio) using a set of primers (Supplemental Table 1). The nucleotide sequences were confirmed with an ABI PRISM 310 genetic analyzer (Applied Biosystems).

The plasmid was transfected into the BL21 (DE3) strain of *Escherichia coli* (Stratagene). The cells were grown at 10°C, and the recombinant protein was induced by treatment with 1.0 mM isopropyl β-D-thiogalactopyranoside for 24 h. The cells were harvested and lysed in buffer A containing 0.2% lysozyme from chicken egg (Wako). The lysate was applied to a 1.5 × 6.0-cm chelating Sepharose FF column (GE Healthcare). The bound recombinant protein was eluted with 50 mM Tris-HCl buffer, pH 7.0, and 20% (w/v) glycerol containing 250 mM imidazole. The concentration of rKJC1 and rVTC1 was determined by the Bradford method with BSA as the standard (Bradford, 1976). The concentration of rKJC2 was determined based on the color intensity after staining with Coomassie Brilliant Blue R 250 on SDS-PAGE compared with the BSA standard (Laemmli, 1970), as the fraction included other proteins.

Nucleotide sugar synthase activity of the recombinant protein was assayed using 1 mM nucleotide triphosphate and 1 mM monosaccharide 1-P as the substrates. In the assay for NDP-sugar pyrophosphorylase activity, 1 mM NDP-sugar and 1 mM PPi were used as the substrates. GDP-L-Fuc, UDP-Gal, UDP-Glc, UDP-GlcA, UTP, PPi, and L-Fuc-1-P were purchased from Sigma-Aldrich.

Copurification Analysis of FLAG-KJC1 with His_6-VTC1

For the expression of rFLAG-KJC1 in *E. coli*, the His_6 sequence in His_6-KJC1/pET15b was replaced with FLAG sequence using oligonucleotides FLAG-F and FLAG-R (Supplemental Table 1). Crude extracts of $rHis_6$-VTC1 and rFLAG-KJC1 prepared as described above were mixed at 4°C for 1 h and applied onto a chelating Sepharose FF column. The column was first washed with 50 mM Tris-HCl buffer, pH 7.0, and 20% (w/v) glycerol, and then with the same buffer containing 250 mM NaCl. The $rHis_6$-VTC1 was eluted with the same buffer containing 250 mM imidazole. As a control experiment, rFLAG-KJC1 alone was also applied to the column and eluted. The fractions obtained were subjected to SDS-PAGE, and $rHis_6$-VTC1 and copurified rFLAG-KJC1 were detected with monoclonal antibodies against His_6 (1:2000 dilution, anti-His-tag pAb; MBL) and FLAG (1:10,000 dilution; anti DYKDDDK tag; Wako), respectively.

Y2H Assay for the Interaction of KJC Proteins with VTC1

The Y2H assay for the detection of the interaction between KJC proteins and VTC1 was performed with the Matchmaker Gold Yeast Two-Hybrid system (Clontech). The full-length CDSs of *KJC1*, *KJC2*, and *VTC1* were amplified from the pET15b plasmids using primer sets KJC1-cDNA-NdeI-F and KJC1-cDNA-BglII-R for *KJC1*, KJC2-cDNA-EcoRI-F and KJC2-cDNA-BamHI-R for *KJC2*, USP-cDNA-EcoRI-F and USP-cDNA-BamHI-R for *USP*, and VTC1-cDNA-EcoRI-F and VTC1-cDNA-BamHI-R for *VTC1* and subcloned into the multicloning sites (KJC1, *Nde*I and *Bam*HI; KJC2, USP, and VTC1, *Eco*RI and *Bam*HI) of bait vector pGADT7 and prey vector pGBKT7. Empty bait and prey plasmids were used for the negative control. According to the manufacturer's instructions, yeast cells (Y2HGold strain; Clontech) were transformed with the bait and prey plasmids and grown on synthetically defined (SD) medium lacking Leu and Trp to confirm the transformation with both bait and prey plasmids and on SD medium lacking His, Leu, and Trp to detect the interaction (Bartel et al., 1993).

Determination of AsA Level in Arabidopsis

The AsA level in Arabidopsis seedlings grown on MS-agar medium for 10 d and on agar for 4 d was determined by the method of Bradley et al. (1973) using a vitamin C assay kit (Cosmo Bio).

Glucomannan Analysis by PACE

AIR was prepared as described (Fry, 2001; Harholt et al., 2006). Briefly, Arabidopsis seedlings grown for 2 weeks (~0.2 g) were treated with 96% (v/v) ethanol at 70°C for 30 min and homogenized using a mortar and pestle. After centrifugation, the precipitate was washed twice with 100% (v/v) ethanol, twice with methanol/chloroform (2:3), and then with 100% (v/v) ethanol, 65% (v/v) ethanol, 80% (v/v) ethanol, and 100% (v/v) ethanol. The sample was lyophilized and used as AIR.

PACE was performed as described (Goubet et al., 2002, 2009). The AIR was treated with aqueous ammonia (200 μL, 30 min) and dried in vacuo. These samples were hydrolyzed into the oligosaccharides with excess β-mannanases Man5A and Man26A from *Pseudomonas fluorescens* (~5 μg each) at room temperature (23°C) overnight in 500 μL of 100 mM ammonium acetate buffer (pH 6.0). Samples and standards [$(Man)_{1-6}$; Megazyme] were derivatized with 8-aminonapthalene-1,3,6-trisulphonic acid, resuspended in urea [6 M for $(Man)_{1-6}$; 2 M for all other materials], and separated by electrophoresis as described (Goubet et al., 2003) with minor modifications to the derivatization process. Gels were visualized using a G-Box (Syngene) with a transilluminator with long-wave tubes emitting at 365 nm and a short-pass (500 to 600 nm) detection filter.

Sugar Composition Analysis of Cell Walls

In this study, sulfuric acid was used for complete hydrolysis of glucomannan. Arabidopsis seedlings were homogenized with a mortar and pestle in 20 mM sodium phosphate buffer (pH 7.0) at 4°C. After centrifugation at 10,000*g* for 5 min and washing twice with water, the precipitate was treated twice with a total 1 mL of 17.5% (w/v) sodium hydroxide and 0.04% (w/v) sodium borohydride for 5 min each and centrifuged to collect soluble cell wall polysaccharides. The soluble polysaccharides were neutralized with 0.5 mL of glacial acetic acid, dialyzed against water at 4°C for 2 d, and lyophilized. The insoluble polysaccharides obtained as the precipitate were washed twice with water, twice with ethanol, twice with ethanol:diethylether (1:1), and with diethylether and then lyophilized. The both polysaccharide fractions were hydrolyzed with 72% (v/v) sulfuric acid at 4°C for 1 h, followed by heating in diluted (8%, v/v) acid solution at 100°C for 4 h, then neutralized with barium carbonate and desalted with Dowex 50W (H^+) resins. Quantification of monosaccharides of cell wall polysaccharides was performed by high-performance anion-exchange chromatography with pulsed amperometric detection using a Dionex DX-500 liquid chromatograph fitted with a CarboPac PA-1 column (Dionex) and a pulsed amperometric detector (Dionex) as described previously (Ishikawa et al., 2000). The sugar composition of total cell walls was calculated based on the sum of soluble (alkali-extracted fraction) and insoluble (the residual fraction) polysaccharides.

NDP-Sugar Analysis by LC-MS/MS

Callus grown in liquid culture was generated and maintained as described previously (Prime et al., 2000). NDP-sugars were extracted according to a previously described method (Lunn et al., 2006) with slight modifications. Lyophilized callus (10 to 15 mg) was ground to a fine powder in liquid nitrogen using a ball mill. Then, 75 μL of chloroform, 175 μL of methanol, and 1 nmol of TDP-Glc (Sigma-Aldrich) as an internal standard was added to the frozen powder, and the samples were thoroughly vortexed. Following incubation at 4°C for 2 h, 400 μL of water was added to each sample, which was mixed by vortexing and centrifuged at 14,000*g* at 4°C for 5 min. The upper aqueous phase was collected and the lower chloroform phase was reextracted twice with 400 μL of water following the same procedures described above. The extracts were combined, dried with a centrifugal vacuum concentrator, and resuspended in 1 mL of water. Solid-phase extraction with Supelclean ENVI-Carb SPE tubes (Sigma-Aldrich) was performed as described by Behmüller et al. (2014). Samples were dried

using a centrifugal vacuum concentrator, resuspended in 500 μL of water, and analyzed immediately. Nucleotide sugars were separated with a porous graphitic carbon LC column (5-μm particle size, 1 × 150 mm; ThermoFisher Scientific) connected to a Uniguard Holder (ThermoFisher Scientific) containing the corresponding guard cartridge (5-μm particle size, 1 × 10 mm; ThermoFisher Scientific) using an Agilent 1100 Series HPLC. Nucleotide sugars were detected using a 4000 QTRAP (AB Sciex) with a Turbo V Ion Source (AB Sciex) exactly as described by Rautengarten et al. (2014). Mass spectrometry parameters for TDP-Glc (Q1 mass, 563 D; Q3 mass, 321 D; collision energy, 30 eV) were determined using direct infusion of 1 μM of TDP-Glc in 50% (v/v) acetonitrile into the electrospray ion source using a syringe pump at a flow rate of 20 μL/min. Nucleotide sugar abundance was determined by signal peak area integration using MultiQuant 2.1 (AB Sciex).

GIPC Analysis

Total sphingolipids including GIPCs were prepared from calli of the wild-type plant and *kjc1-1* and *kjc2-1* mutants and analyzed by LC-MS/MS as described (Nagano et al., 2014). Peaks of GIPCs with different hexose numbers (Hex_0, Hex_1, and Hex_2) were assigned based on multiple reaction monitoring transitions (Mortimer et al., 2013).

Phylogenetic Analysis

The amino acid sequences of nucleotide sugar pyrophosphorylases in Arabidopsis were obtained from TAIR, and those in other organisms from NCBI BLAST (blast.ncbi.nlm.nih.gov/Blast.cgi) using BLASTP searches. The alignments of amino acid sequences were performed using the MUSCLE program in MEGA software (version 6; Tamura et al., 2013) with default parameters other than Gap Open (-2.5). The phylogenetic trees were generated using the neighbor-joining method with 1000 bootstrap replications. To optimize the alignment, GDP-L-Fuc pyrophosphorylase regions of At1g01220.1 (Trp^{34}-Leu^{565}) and Os03g0115100 (Trp^{44}-Leu^{588}) were used in the analysis shown in Figure 1A.

Accession Numbers

Sequence data from this article can be found in TAIR or GenBank/EMBL libraries under the accession numbers listed in Supplemental Table 3.

Supplemental Data

Supplemental Figure 1. The Man/L-Gal pathway for the generation of AsA in plants.

Supplemental Figure 2. Alignment of amino acid sequences of GMPPs and KJC proteins.

Supplemental Figure 3. Arabidopsis T-DNA insertion lines for *KJC* genes.

Supplemental Figure 4. GMPP activity in *kjc* mutants and *KJC*-overexpressing plants.

Supplemental Figure 5. Complementation of *kjc1-1* mutant with genomic *KJC1* gene.

Supplemental Figure 6. Expression patterns of *KJC1*, *KJC2*, and *VTC1*.

Supplemental Figure 7. Expression of *KJC1*, *KJC2*, and *VTC1* in *kjc* mutants and *KJC*-overexpressing plants.

Supplemental Figure 8. Seed development in *kjc* mutants.

Supplemental Figure 9. Protein gel blot analysis of *N*-glycans of glycoproteins.

Supplemental Figure 10. Sugar composition of GIPC in calli of *kjc* mutants.

Supplemental Figure 11. Preparation of native and point-mutated recombinant proteins.

Supplemental Figure 12. KJC/GMPP subunit α and VTC1/GMPP subunit β subfamilies.

Supplemental Figure 13. Interaction of KJC1 with USP in yeast cells.

Supplemental Table 1. Sequences of primers used in the present study.

Supplemental Table 2. Substrate specificity of rVTC1 in the absence and presence of rKJCs.

Supplemental Table 3. Accession numbers for amino acid sequences.

Supplemental File 1. Phylogenetic relationships shown in Figure 1.

Supplemental File 2. Phylogenetic relationships shown in Supplemental Figure 12.

ACKNOWLEDGMENTS

We thank O. Kosik (Rothamsted Research, UK) for valuable discussion on NDP-sugar analysis. This work was financially supported in part by a Grant-in-Aid for Scientific Research to T.K. (22770030) from the Japan Society of the Promotion of Science, and by Grant-in-Aid for Scientific Research (24114006) to Y.T. and T.K. from the Ministry of Education, Culture, Sports, Science, and Technology of Japan. Support was also provided by the BBSRC Sustainable Bioenergy Centre: Cell wall sugars programme to P.D. (Grant BB/G016240/1) and by the RIKEN Foreign Postdoctoral Research program to J.C.M. J.C.M.'s work at the Joint BioEnergy Institute was supported by the Office of Science, Office of Biological and Environmental Research of the U.S. Department of Energy under Contract DE-AC02-05CH11231.

AUTHOR CONTRIBUTIONS

J.C.M., P.D., Y.T., and T.K. designed the experimental strategies. S.S., N.T., and Y. Yamanashi measured GDP-Man pyrophosphorylase activity and L-ascorbic acid level in *kjc* mutants and *KJC*-overexpressing plants. T.I. and M. K.-Y. analyzed sphingolipids in the mutants. J.C.M., X.Y., and J.L. performed NDP-sugar analysis. N.T., J.C.M., and X.Y. analyzed cell wall polysaccharides. S.S, N.T., Y. Yamanashi, Y. Yoshimi, and T.K. characterized recombinant proteins and carried out Y2H and copurification experiments. J.C.M., X.Y., J.L., T.I., Y. Yoshimi, and T.K. analyzed the data. J.C.M., P.D., Y.T., and T.K. wrote the article.

Received June 1, 2015; revised November 6, 2015; accepted November 24, 2015; published December 15, 2015.

REFERENCES

Bartel, P.L., Chien, C.-T., Sternglanz, R., and Fields, S. (1993). Using the two-hybrid system to detect protein-protein interactions. In Cellular Interactions in Development: A Practical Approach, D.A. Hartley, ed (Oxford, UK: Oxford University Press), pp. 153–179.

Behmüller, R., Forstenlehner, I.C., Tenhaken, R., and Huber, C.G. (2014). Quantitative HPLC-MS analysis of nucleotide sugars in plant

cells following off-line SPE sample preparation. Anal. Bioanal. Chem. **406:** 3229–3237.

Bradford, M.M. (1976). A rapid and sensitive method for the quantitation of microgram quantities of protein utilizing the principle of protein-dye binding. Anal. Biochem. **72:** 248–254.

Bradley, D.W., Emery, G., and Maynard, J.E. (1973). Vitamin C in plasma: a comparative study of the vitamin stabilized with trichloroacetic acid or metaphosphoric acid and the effects of storage at -70°, -20°, 4°, and 25° on the stabilized vitamin. Clin. Chim. Acta **44:** 47–52.

Clough, S.J., and Bent, A.F. (1998). Floral dip: a simplified method for *Agrobacterium*-mediated transformation of *Arabidopsis thaliana.* Plant J. **16:** 735–743.

Cocuron, J.C., Lerouxel, O., Drakakaki, G., Alonso, A.P., Liepman, A.H., Keegstra, K., Raikhel, N., and Wilkerson, C.G. (2007). A gene from the cellulose synthase-like C family encodes a β-1,4 glucan synthase. Proc. Natl. Acad. Sci. USA **104:** 8550–8555.

Conklin, P.L., Norris, S.R., Wheeler, G.L., Williams, E.H., Smirnoff, N., and Last, R.L. (1999). Genetic evidence for the role of GDP-mannose in plant ascorbic acid (vitamin C) biosynthesis. Proc. Natl. Acad. Sci. USA **96:** 4198–4203.

Conklin, P.L., Pallanca, J.E., Last, R.L., and Smirnoff, N. (1997). L-ascorbic acid metabolism in the ascorbate-deficient Arabidopsis mutant *vtc1.* Plant Physiol. **115:** 1277–1285.

Crevillén, P., Ballicora, M.A., Mérida, A., Preiss, J., and Romero, J.M. (2003). The different large subunit isoforms of *Arabidopsis thaliana* ADP-glucose pyrophosphorylase confer distinct kinetic and regulatory properties to the heterotetrameric enzyme. J. Biol. Chem. **278:** 28508–28515.

Cronje, C., George, G.M., Fernie, A.R., Bekker, J., Kossmann, J., and Bauer, R. (2012). Manipulation of L-ascorbic acid biosynthesis pathways in *Solanum lycopersicum*: elevated GDP-mannose pyrophosphorylase activity enhances L-ascorbate levels in red fruit. Planta **235:** 553–564.

Davis, J., Brandizzi, F., Liepman, A.H., and Keegstra, K. (2010). Arabidopsis mannan synthase CSLA9 and glucan synthase CSLC4 have opposite orientations in the Golgi membrane. Plant J. **64:** 1028–1037.

Dowdle, J., Ishikawa, T., Gatzek, S., Rolinski, S., and Smirnoff, N. (2007). Two genes in *Arabidopsis thaliana* encoding GDP-L-galactose phosphorylase are required for ascorbate biosynthesis and seedling viability. Plant J. **52:** 673–689.

Faye, L., Gomord, V., Fitchette-Lainé, A.C., and Chrispeels, M.J. (1993). Affinity purification of antibodies specific for Asn-linked glycans containing α 1–>3 fucose or β 1–>2 xylose. Anal. Biochem. **209:** 104–108.

Fraga, C.G., Motchnik, P.A., Shigenaga, M.K., Helbock, H.J., Jacob, R.A., and Ames, B.N. (1991). Ascorbic acid protects against endogenous oxidative DNA damage in human sperm. Proc. Natl. Acad. Sci. USA **88:** 11003–11006.

Fry, S. (2001). Chemical and Metabolic Analysis. (Caldwell, NJ: The Blackburn Press).

Gilbert, L., et al. (2009). GDP-D-mannose 3,5-epimerase (GME) plays a key role at the intersection of ascorbate and non-cellulosic cell-wall biosynthesis in tomato. Plant J. **60:** 499–508.

Gordon, R., and Maclachlan, G. (1989). Incorporation of UDP-[^{14}C] glucose into xyloglucan by pea membranes. Plant Physiol. **91:** 373–378.

Goubet, F., Barton, C.J., Mortimer, J.C., Yu, X., Zhang, Z., Miles, G.P., Richens, J., Liepman, A.H., Seffen, K., and Dupree, P. (2009). Cell wall glucomannan in Arabidopsis is synthesised by CSLA glycosyltransferases, and influences the progression of embryogenesis. Plant J. **60:** 527–538.

Goubet, F., Jackson, P., Deery, M.J., and Dupree, P. (2002). Polysaccharide analysis using carbohydrate gel electrophoresis: a method to study plant cell wall polysaccharides and polysaccharide hydrolases. Anal. Biochem. **300:** 53–68.

Goubet, F., Misrahi, A., Park, S.K., Zhang, Z., Twell, D., and Dupree, P. (2003). AtCSLA7, a cellulose synthase-like putative glycosyltransferase, is important for pollen tube growth and embryogenesis in Arabidopsis. Plant Physiol. **131:** 547–557.

Harholt, J., Jensen, J.K., Sørensen, S.O., Orfila, C., Pauly, M., and Scheller, H.V. (2006). ARABINAN DEFICIENT 1 is a putative arabinosyltransferase involved in biosynthesis of pectic arabinan in Arabidopsis. Plant Physiol. **140:** 49–58.

Hayashi, T., Read, S.M., Bussell, J., Thelen, M., Lin, F.C., Brown, R.M., and Delmer, D.P. (1987). UDP-glucose: (1→3)-β-glucan synthases from mung bean and cotton: differential effects of Ca^{2+} and Mg^{2+} on enzyme properties and on macromolecular structure of the glucan product. Plant Physiol. **83:** 1054–1062.

Hemavathi, U.C.P., Upadhyaya, C.P., Akula, N., Young, K.E., Chun, S.C., Kim, D.H., and Park, S.W. (2010). Enhanced ascorbic acid accumulation in transgenic potato confers tolerance to various abiotic stresses. Biotechnol. Lett. **32:** 321–330.

Hruz, T., Laule, O., Szabo, G., Wessendorp, F., Bleuler, S., Oertle, L., Widmayer, P., Gruissem, W., and Zimmermann, P. (2008). Genevestigator v3: a reference expression database for the meta-analysis of transcriptomes. Adv. Bioinforma. **2008:** 420747.

Ishikawa, M., Kuroyama, H., Takeuchi, Y., and Tsumuraya, Y. (2000). Characterization of pectin methyltransferase from soybean hypocotyls. Planta **210:** 782–791.

Koehler, K., et al. (2013). Mutations in *GMPPA* cause a glycosylation disorder characterized by intellectual disability and autonomic dysfunction. Am. J. Hum. Genet. **93:** 727–734.

Kotake, T., Hirosawa, C., Ando, Y., and Tsumuraya, Y. (2010). Generation of nucleotide sugars for biomass formation in plants. Plant Biotechnol. **27:** 231–236.

Kotake, T., Hojo, S., Tajima, N., Matsuoka, K., Koyama, T., and Tsumuraya, Y. (2008). A bifunctional enzyme with L-fucokinase and GDP-L-fucose pyrophosphorylase activities salvages free L-fucose in Arabidopsis. J. Biol. Chem. **283:** 8125–8135.

Kotake, T., Hojo, S., Yamaguchi, D., Aohara, T., Konishi, T., and Tsumuraya, Y. (2007). Properties and physiological functions of UDP-sugar pyrophosphorylase in *Arabidopsis.* Biosci. Biotechnol. Biochem. **71:** 761–771.

Kotake, T., Yamaguchi, D., Ohzono, H., Hojo, S., Kaneko, S., Ishida, H.K., and Tsumuraya, Y. (2004). UDP-sugar pyrophosphorylase with broad substrate specificity toward various monosaccharide 1-phosphates from pea sprouts. J. Biol. Chem. **279:** 45728–45736.

Laemmli, U.K. (1970). Cleavage of structural proteins during the assembly of the head of bacteriophage T4. Nature **227:** 680–685.

Liepman, A.H., Wilkerson, C.G., and Keegstra, K. (2005). Expression of cellulose synthase-like (*Csl*) genes in insect cells reveals that *CslA* family members encode mannan synthases. Proc. Natl. Acad. Sci. USA **102:** 2221–2226.

Linster, C.L., Gomez, T.A., Christensen, K.C., Adler, L.N., Young, B.D., Brenner, C., and Clarke, S.G. (2007). Arabidopsis *VTC2* encodes a GDP-L-galactose phosphorylase, the last unknown enzyme in the Smirnoff-Wheeler pathway to ascorbic acid in plants. J. Biol. Chem. **282:** 18879–18885.

Lukowitz, W., Nickle, T.C., Meinke, D.W., Last, R.L., Conklin, P.L., and Somerville, C.R. (2001). *Arabidopsis cyt1* mutants are deficient in a mannose-1-phosphate guanylyltransferase and point to a requirement of N-linked glycosylation for cellulose biosynthesis. Proc. Natl. Acad. Sci. USA **98:** 2262–2267.

Lunn, J.E., Feil, R., Hendriks, J.H., Gibon, Y., Morcuende, R., Osuna, D., Scheible, W.R., Carillo, P., Hajirezaei, M.R., and Stitt, M. (2006). Sugar-induced increases in trehalose 6-phosphate are correlated with redox activation of ADPglucose pyrophosphorylase and higher rates of starch synthesis in *Arabidopsis thaliana.* Biochem. J. **397:** 139–148.

Michael, T.P., et al. (2008). Network discovery pipeline elucidates conserved time-of-day-specific cis-regulatory modules. PLoS Genet. **4:** e14.

Mortimer, J.C., et al. (2013). Abnormal glycosphingolipid mannosylation triggers salicylic acid-mediated responses in *Arabidopsis.* Plant Cell **25:** 1881–1894.

Murad, S., Grove, D., Lindberg, K.A., Reynolds, G., Sivarajah, A., and Pinnell, S.R. (1981). Regulation of collagen synthesis by ascorbic acid. Proc. Natl. Acad. Sci. USA **78:** 2879–2882.

Nagano, M., Ishikawa, T., Ogawa, Y., Iwabuchi, M., Nakasone, A., Shimamoto, K., Uchimiya, H., and Kawai-Yamada, M. (2014). Arabidopsis Bax inhibitor-1 promotes sphingolipid synthesis during cold stress by interacting with ceramide-modifying enzymes. Planta **240:** 77–89.

Ning, B., and Elbein, A.D. (2000). Cloning, expression and characterization of the pig liver GDP-mannose pyrophosphorylase. Evidence that GDP-mannose and GDP-Glc pyrophosphorylases are different proteins. Eur. J. Biochem. **267:** 6866–6874.

Osorio, S., Nunes-Nesi, A., Stratmann, M., and Fernie, A.R. (2013). Pyrophosphate levels strongly influence ascorbate and starch content in tomato fruit. Front. Plant Sci. **4:** 308.

Park, J.I., Ishimizu, T., Suwabe, K., Sudo, K., Masuko, H., Hakozaki, H., Nou, I.S., Suzuki, G., and Watanabe, M. (2010). UDP-glucose pyrophosphorylase is rate limiting in vegetative and reproductive phases in *Arabidopsis thaliana.* Plant Cell Physiol. **51:** 981–996.

Pastori, G.M., Kiddle, G., Antoniw, J., Bernard, S., Veljovic-Jovanovic, S., Verrier, P.J., Noctor, G., and Foyer, C.H. (2003). Leaf vitamin C contents modulate plant defense transcripts and regulate genes that control development through hormone signaling. Plant Cell **15:** 939–951.

Pauly, M., Porchia, A., Olsen, C.E., Nunan, K.J., and Scheller, H.V. (2000). Enzymatic synthesis and purification of uridine diphospho-β-l-arabinopyranose, a substrate for the biosynthesis of plant polysaccharides. Anal. Biochem. **278:** 69–73.

Petreikov, M., Eisenstein, M., Yeselson, Y., Preiss, J., and Schaffer, A.A. (2010). Characterization of the AGPase large subunit isoforms from tomato indicates that the recombinant L3 subunit is active as a monomer. Biochem. J. **428:** 201–212.

Prime, T.A., Sherrier, D.J., Mahon, P., Packman, L.C., and Dupree, P. (2000). A proteomic analysis of organelles from *Arabidopsis thaliana.* Electrophoresis **21:** 3488–3499.

Rautengarten, C., et al. (2014). The Golgi localized bifunctional UDP-rhamnose/UDP-galactose transporter family of *Arabidopsis.* Proc. Natl. Acad. Sci. USA **111:** 11563–11568.

Reiter, W.-D. (2008). Biochemical genetics of nucleotide sugar interconversion reactions. Curr. Opin. Plant Biol. **11:** 236–243.

Reiter, W.-D., and Vanzin, G.F. (2001). Molecular genetics of nucleotide sugar interconversion pathways in plants. Plant Mol. Biol. **47:** 95–113.

Scheller, H.V., and Ulvskov, P. (2010). Hemicelluloses. Annu. Rev. Plant Biol. **61:** 263–289.

Schnurr, J.A., Storey, K.K., Jung, H.J., Somers, D.A., and Gronwald, J.W. (2006). UDP-sugar pyrophosphorylase is essential for pollen development in Arabidopsis. Planta **224:** 520–532.

Szumilo, T., Drake, R.R., York, J.L., and Elbein, A.D. (1993). GDP-mannose pyrophosphorylase. Purification to homogeneity, properties, and utilization to prepare photoaffinity analogs. J. Biol. Chem. **268:** 17943–17950.

Tamura, K., Stecher, G., Peterson, D., Filipski, A., and Kumar, S. (2013). MEGA6: Molecular evolutionary genetics analysis version 6.0. Mol. Biol. Evol. **30:** 2725–2729.

Torabinejad, J., Donahue, J.L., Gunesekera, B.N., Allen-Daniels, M.J., and Gillaspy, G.E. (2009). VTC4 is a bifunctional enzyme that affects myoinositol and ascorbate biosynthesis in plants. Plant Physiol. **150:** 951–961.

Tóth, S.Z., Nagy, V., Puthur, J.T., Kovács, L., and Garab, G. (2011). The physiological role of ascorbate as photosystem II electron donor: protection against photoinactivation in heat-stressed leaves. Plant Physiol. **156:** 382–392.

Untergasser, A., Cutcutache, I., Koressaar, T., Ye, J., Faircloth, B.C., Remm, M., and Rozen, S.G. (2012). Primer3–new capabilities and interfaces. Nucleic Acids Res. **40:** e115.

Vacca, R.A., de Pinto, M.C., Valenti, D., Passarella, S., Marra, E., and De Gara, L. (2004). Production of reactive oxygen species, alteration of cytosolic ascorbate peroxidase, and impairment of mitochondrial metabolism are early events in heat shock-induced programmed cell death in tobacco Bright-Yellow 2 cells. Plant Physiol. **134:** 1100–1112.

Voxeur, A., Gilbert, L., Rihouey, C., Driouich, A., Rothan, C., Baldet, P., and Lerouge, P. (2011). Silencing of the GDP-D-mannose 3,5-epimerase affects the structure and cross-linking of the pectic polysaccharide rhamnogalacturonan II and plant growth in tomato. J. Biol. Chem. **286:** 8014–8020.

Wang, J., Yu, Y., Zhang, Z., Quan, R., Zhang, H., Ma, L., Deng, X.W., and Huang, R. (2013b). *Arabidopsis* CSN5B interacts with VTC1 and modulates ascorbic acid synthesis. Plant Cell **25:** 625–636.

Wang, Y., Mortimer, J.C., Davis, J., Dupree, P., and Keegstra, K. (2013a). Identification of an additional protein involved in mannan biosynthesis. Plant J. **73:** 105–117.

Wheeler, G.L., Jones, M.A., and Smirnoff, N. (1998). The biosynthetic pathway of vitamin C in higher plants. Nature **393:** 365–369.

Winter, D., Vinegar, B., Nahal, H., Ammar, R., Wilson, G.V., and Provart, N.J. (2007). An "Electronic Fluorescent Pictograph" browser for exploring and analyzing large-scale biological data sets. PLoS One **2:** e718.

Wolucka, B.A., and Van Montagu, M. (2007). The VTC2 cycle and the de novo biosynthesis pathways for vitamin C in plants: an opinion. Phytochemistry **68:** 2602–2613.

Zhang, Z., Wang, J., Zhang, R., and Huang, R. (2012). The ethylene response factor AtERF98 enhances tolerance to salt through the transcriptional activation of ascorbic acid synthesis in Arabidopsis. Plant J. **71:** 273–287.